Supporting Information

Electron oriented injection $TiSe_2$-C laminated heterojunctions derived from terminal functionalized MXene for high-rate sodium ion storage

Enze Xu,[a] Jiamin Zhang,[a] Yishao Liu,[a] Hanwen Zhu,[a] Zhenjie Sun,[a] Yajing Chang,[b] Guoqing Tong, *[a] Dabin Yu,[b] Yang Jiang*[a]

[a]School of Materials Science and Engineering, Hefei University of Technology, 230009, Hefei, People's Republic of China

Corresponding author: apjiang@hfut.edu.cn; tnggq11@163.com

[b]State Key Laboratory of Pulsed Power Laser Technology, National University of Defense Technology, 230037, Hefei, People's Republic of China

Experiment Section

Materials

Hydrofluoric acid (HF), Lithium fluoride (LiF), Hydrochloric acid (HCl), Cupric chloride ($CuCl_2$), Ammonium hydroxide ($NH_3 \cdot H_2O$), and Ammonium chloride (NH_4Cl) were purchased from Shanghai Aladdin Bio-Chem Technology Co., LTD. Ti_3AlC_2 (400 mesh) was purchased from Jilin 11 technology Co., LTD. All reagents were used without further treatment.

Synthesis of MXene

According to previous reports, $Ti_3C_2Cl_2$ MXene was synthesized by the molten etching method.[1] 1 mmol Ti_3AlC_2, and 4 mmol $CuCl_2$ was mixed uniformly by the mortar in a glovebox filled with Ar atmosphere. Then, the mixed powder was poured into a corundum crucible and transferred into tube furnace quickly. The sample was heated at 700 ℃ for 7 h with a heating rate of 2 ℃/min. The final product was stirred in a

$NH_4Cl/NH_3{\cdot}H_2O$ (1/1 in vol) solution for 2 h, and washed with DI water until PH reached to 7. $Ti_3C_2T_x$ (T= O, F, OH) MXene was synthesized by HF etching method.[2]

Synthesis of $TiSe_2$-Cl and $TiSe_2$-F

A traditional solid-state reaction was adopted to synthesis $TiSe_2$. 1 mmol MXene was mixed with 2 mmol Selenium (Se) powders by the mortar. Then, the mixture was loaded into a quartz glass tube (120 mm length, 8 mm diameter) and pumped to 10 Pa. The sealed tube was sintered in a furnace at 575 ℃ for 48 h.

Materials Characterization

X-ray diffraction (XRD) patterns were performed by Rigaku SmartLab X-ray diffractometer equipped with Cu Kα radiation. Scanning electron microscope (SEM) images were measured by ZEISS Gemini 500 equipped with EDS system. Transmission electron microscope (TEM) photographs were performed in JEM-2100F. Raman spectrogram were collected by HORIBA JOBIN YVON Ramoscope system with 633 nm laser. X-ray photoelectron spectroscopy (XPS) data were obtained by Thermo Scientific ESCALAB 250Xi. Thermogravimetric analysis (TGA) was tested by NETZSCH STA 449 F3 Jupiter® from RT to 800 ℃.

Electrochemical Performances

The $TiSe_2$ based cathode electrode was prepared by mixing active materials, Super P and PVDF with a mass ratio of 8:1:1 in NMP with the associated of homogenizer. The sticky paste was coated on the Copper foil by the blade, and the mass loading of active materials was about 1 mg cm^{-2}. 1.0M $NaPF_6$ in DIGLYME was used as electrolyte. Cyclic voltammetry (CV) curves from 0.1 – 3 V were measured by CHI 660D electrochemical

workstation. Galvanostatic charge/discharge (GCD) performances were performed by Neware BTS 4001 test platforms. Electrochemical impedance spectroscopy (EIS) was carried by Zahner Zennium workstation in the range of 0.01 Hz to 100 MHz.

DFT Calculation

All theorical simulations were carried out with Quantum ESPRESSO v6.4.1 software packages.[3] Perdew-Burke-Ernzerh (PBE) in generalized gradient approximation (GGA) considering Van der Waals force (VDW) was employed to analyze the exchange functional.[4] Monkhorst−Pack k-point mesh was 3×3×1. The kinetic energy cutoffs for the wavefunction was 60 Ry. For all heterojunction structure, the energy convergence accuracy was1×10^{-8} eV, and the force tolerance for geometry optimization was 0.005 eV/Å. Climbing image nudged elastic band (CI-NEB) method was adopted to analysis the energy barrier of sodium ion in heterojunction.[5]

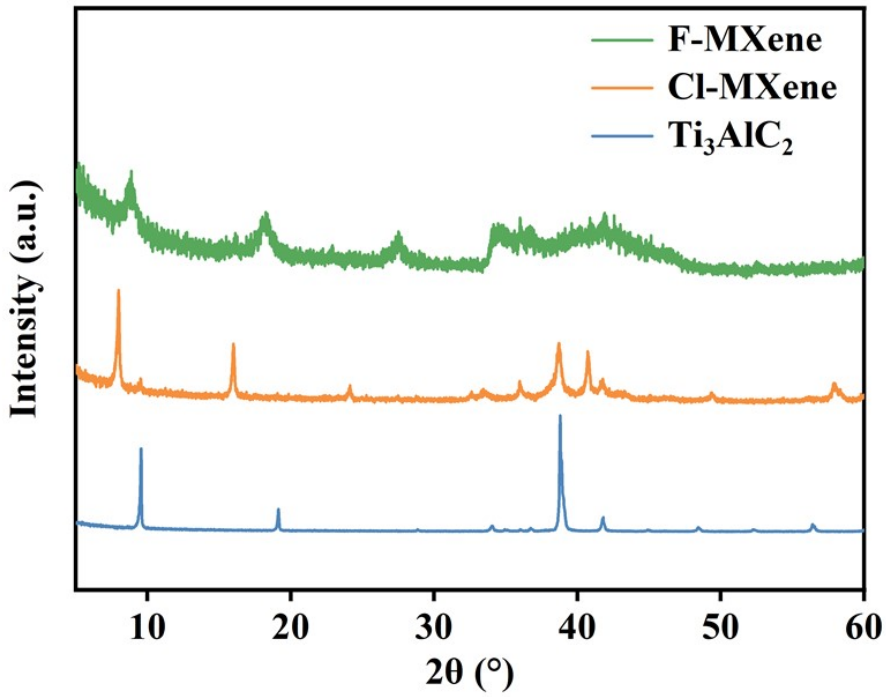

Figure S1. XRD patterns of Ti_3AlC_2, Cl-MXene, and F-MXene.

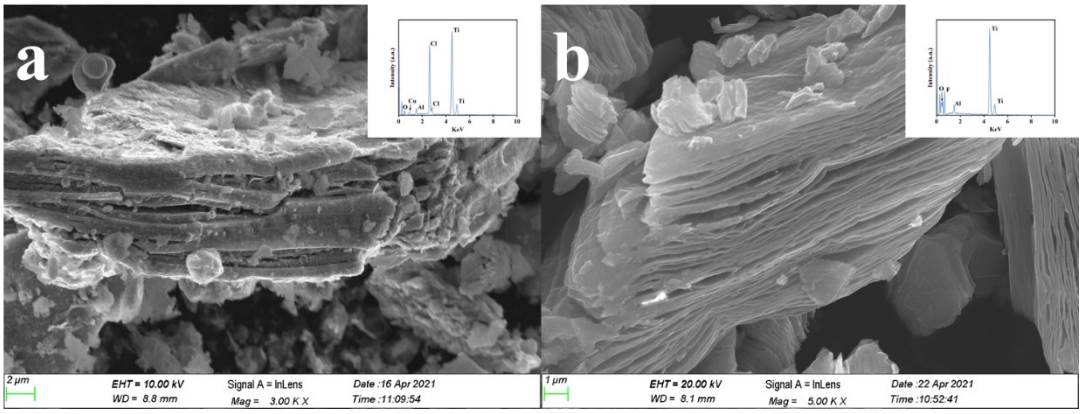

Figure S2. SEM images and EDS analysis of (a) Cl-MXene, (b) F-MXene.

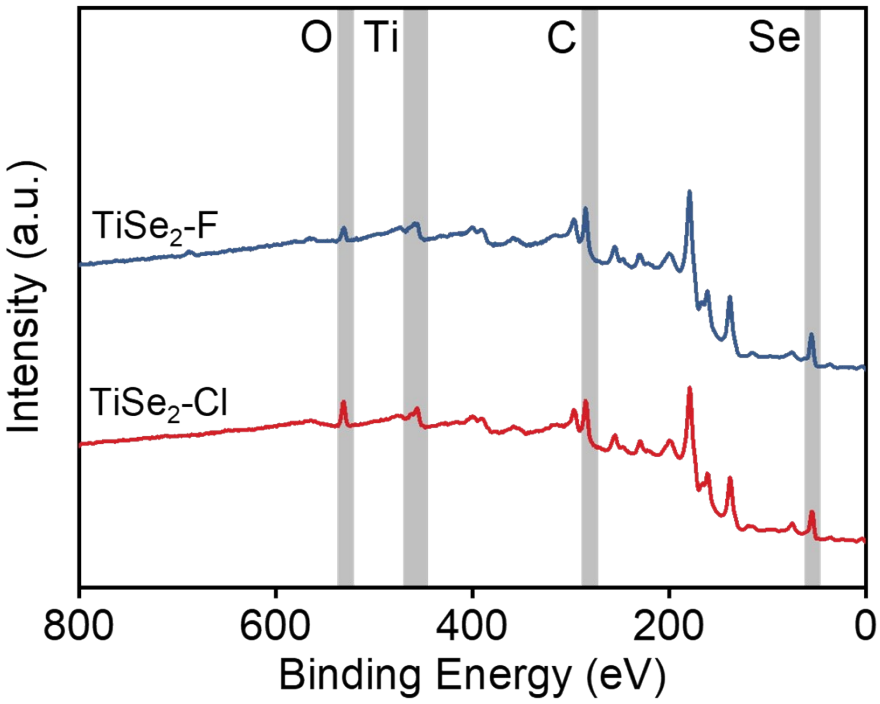

Figure S3. Total XPS spectra of $TiSe_2$-Cl, and $TiSe_2$-F.

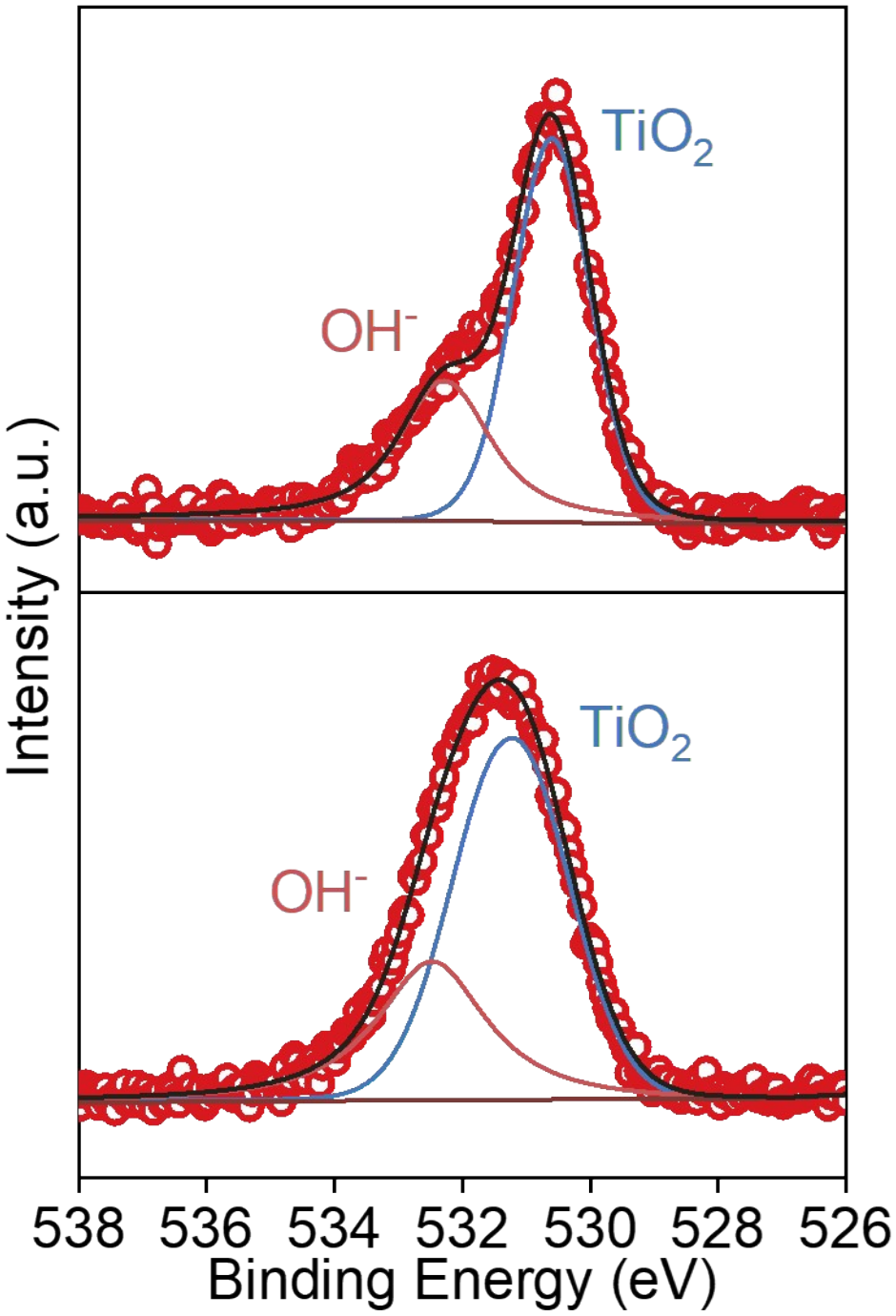

Figure S4. XPS spectra of O 1s for $TiSe_2$-Cl and $TiSe_2$-F.

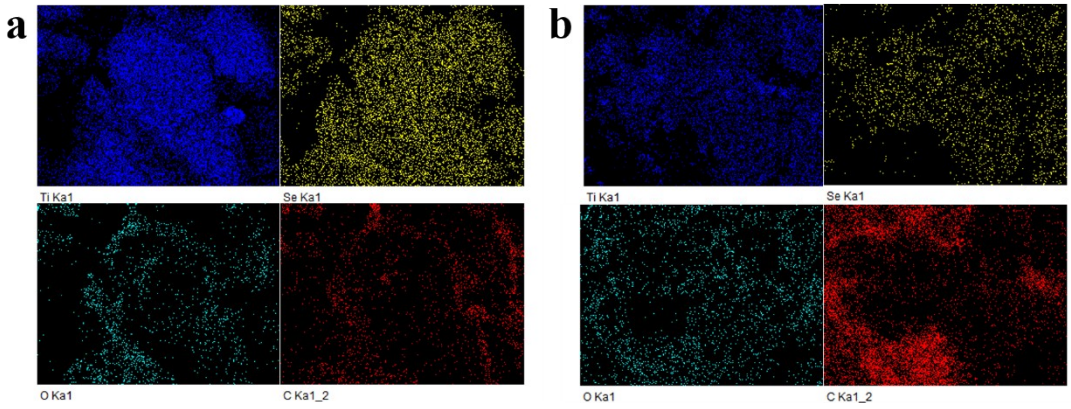

Figure S5. EDX mapping analysis of (a) $TiSe_2$-Cl, (b) $TiSe_2$-F.

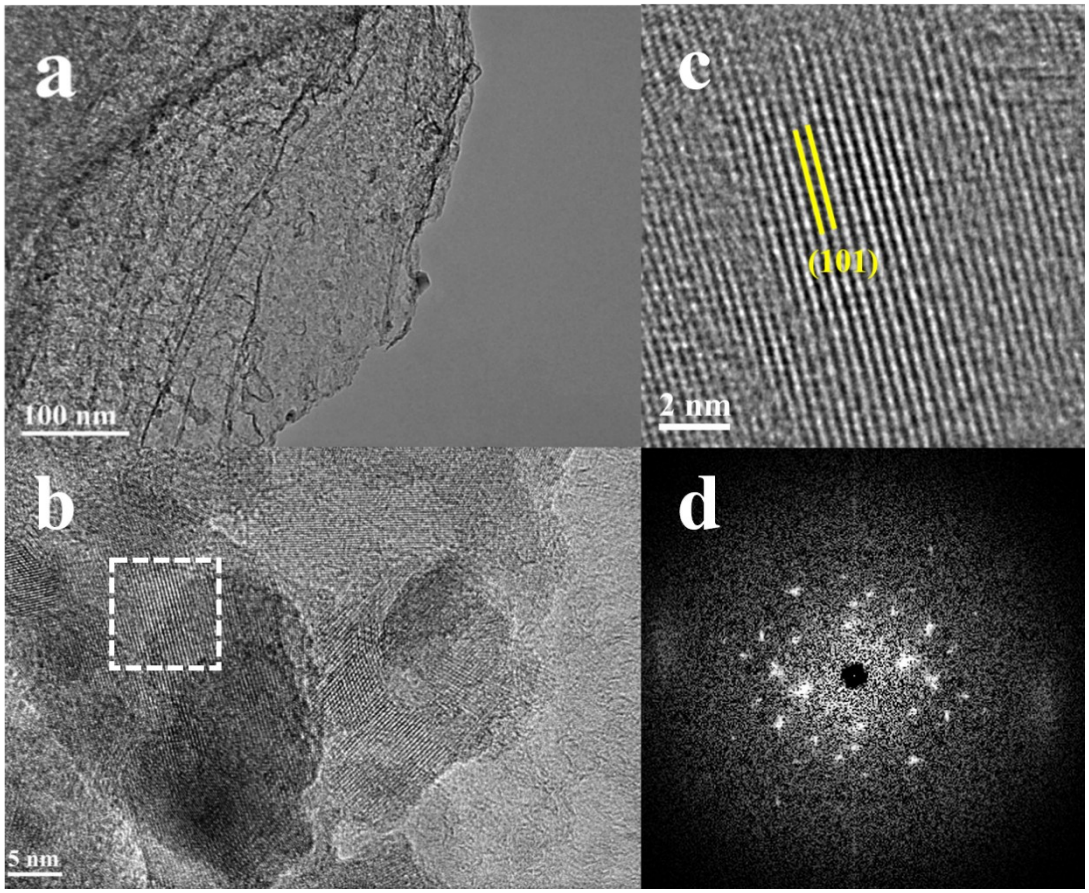

Figure S6. (a) TEM images of amorphous carbon, (b, c) HRTEM of $TiSe_2$-F, (d) FFT image of (c).

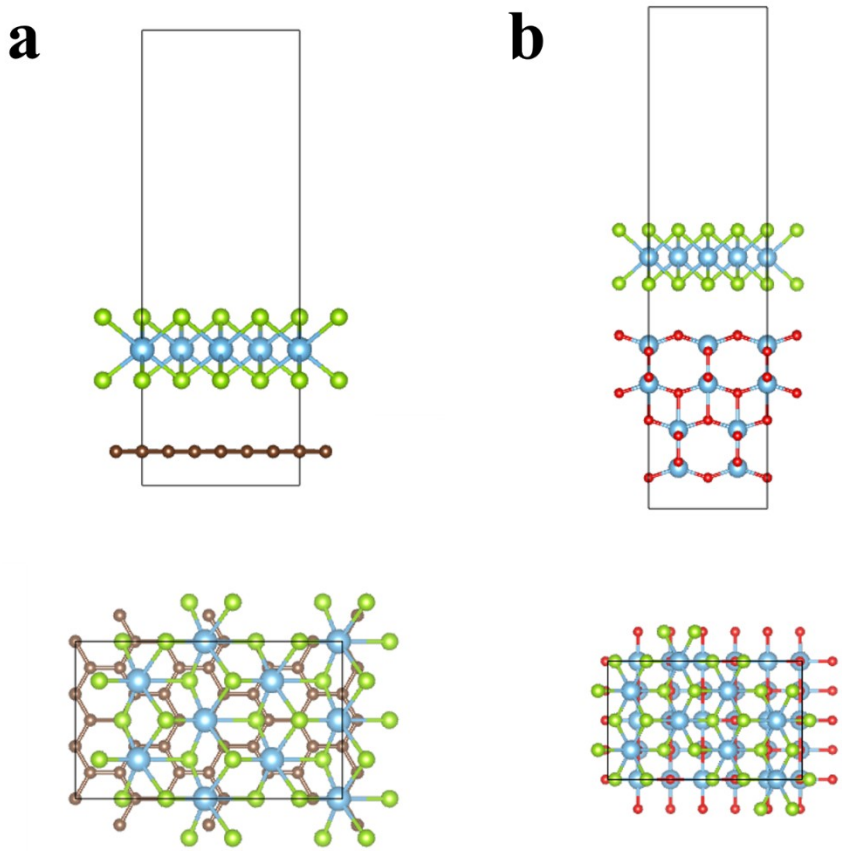

Figure S7. Crystal model of (a) $TiSe_2$-C, (b) $TiSe_2$-TiO_2 heterojunction after relaxation

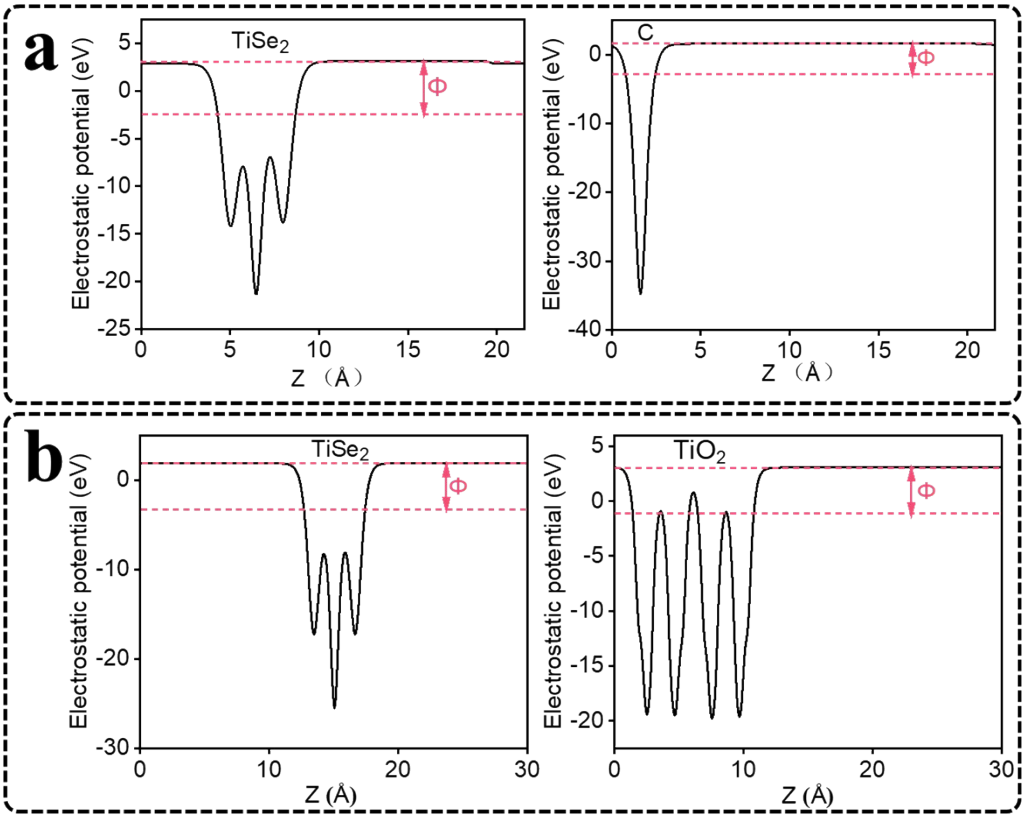

Figure S8. Work function of (a) $TiSe_2$ and C in $TiSe_2$-C, (b) $TiSe_2$ and TiO_2 in $TiSe_2$-TiO_2 heterojunction.

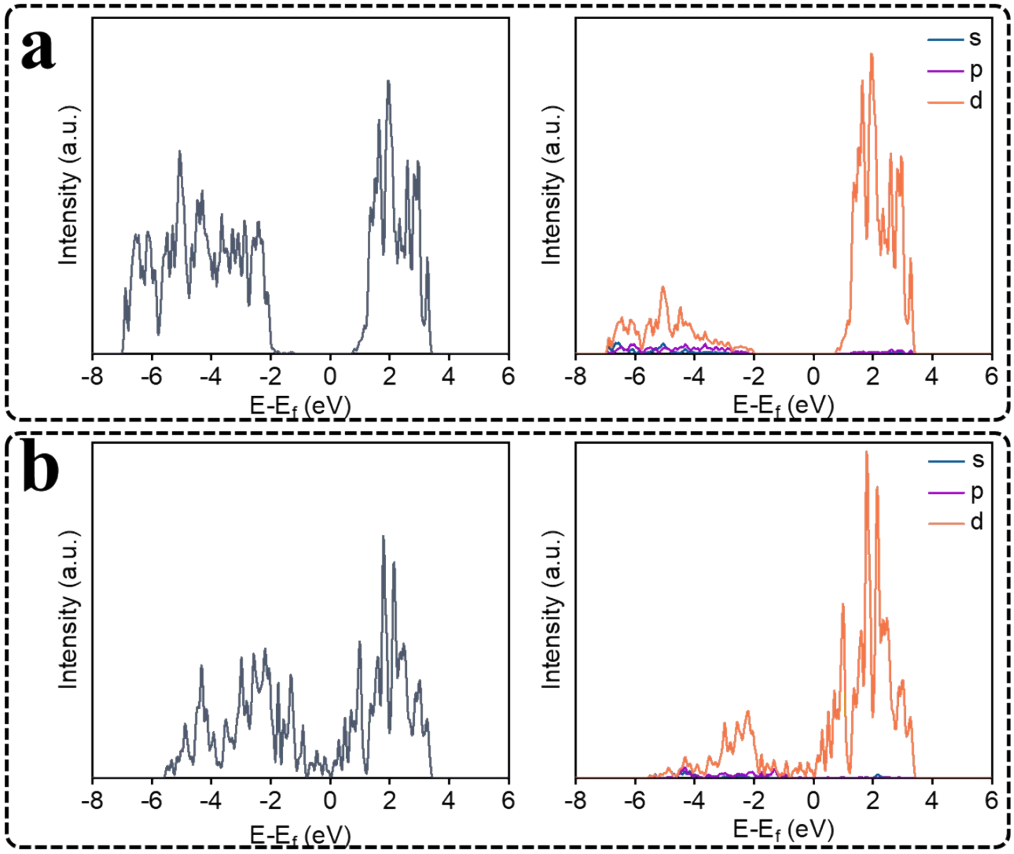

Figure S9. (a) DOS analysis of TiO_2, and PDOS of Ti in TiO_2, (b) DOS analysis of $TiSe_2$, and PDOS of Ti in $TiSe_2$ in $TiSe_2$-TiO_2 heterojunction.

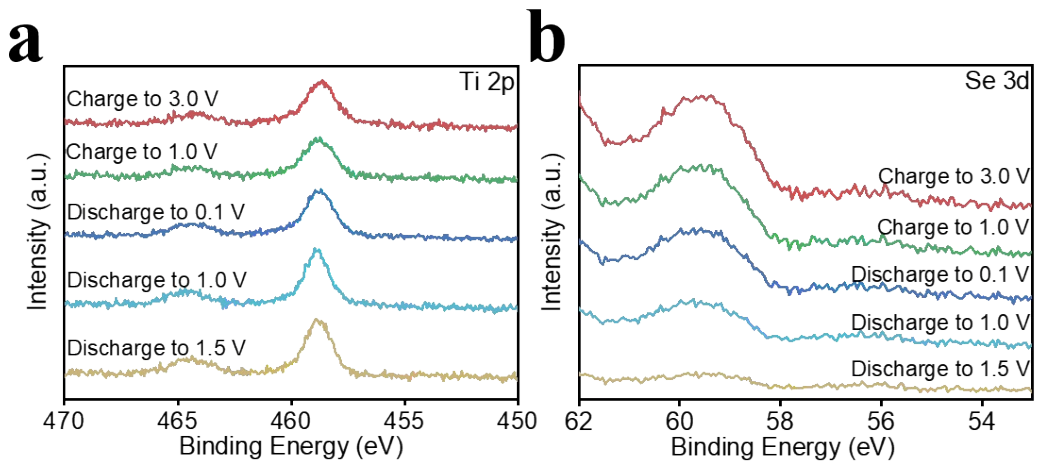

Figure S10. Ex-situ XPS analysis of (a) Ti 2p, (b) Se 3d of $TiSe_2$-F.

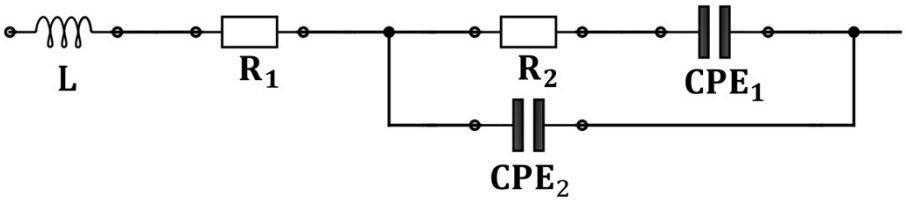

Figure S11. Fitting equivalent circuit diagram of EIS.

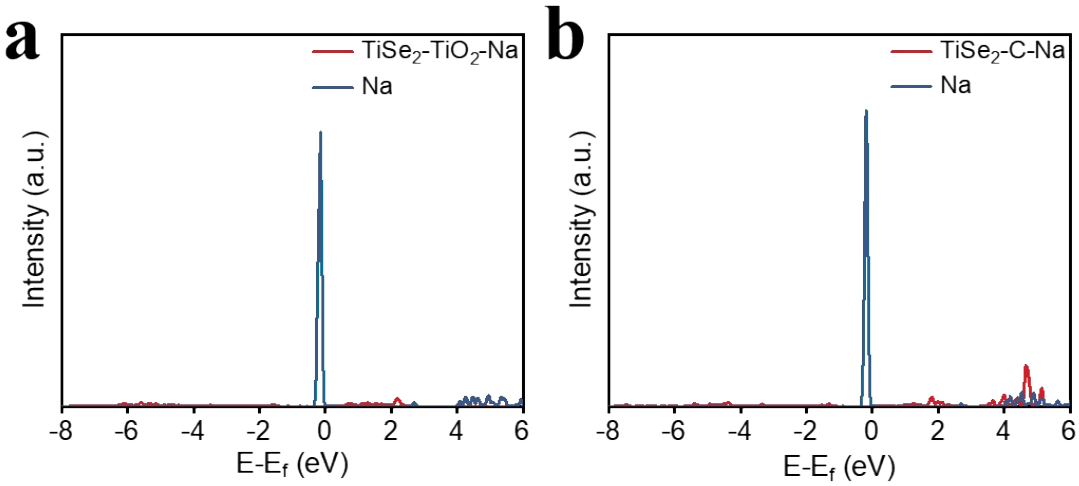

Figure S12. s orbital analysis of (a) Na in $TiSe_2$-TiO_2-Na, (b) Na in $TiSe_2$-C-Na.

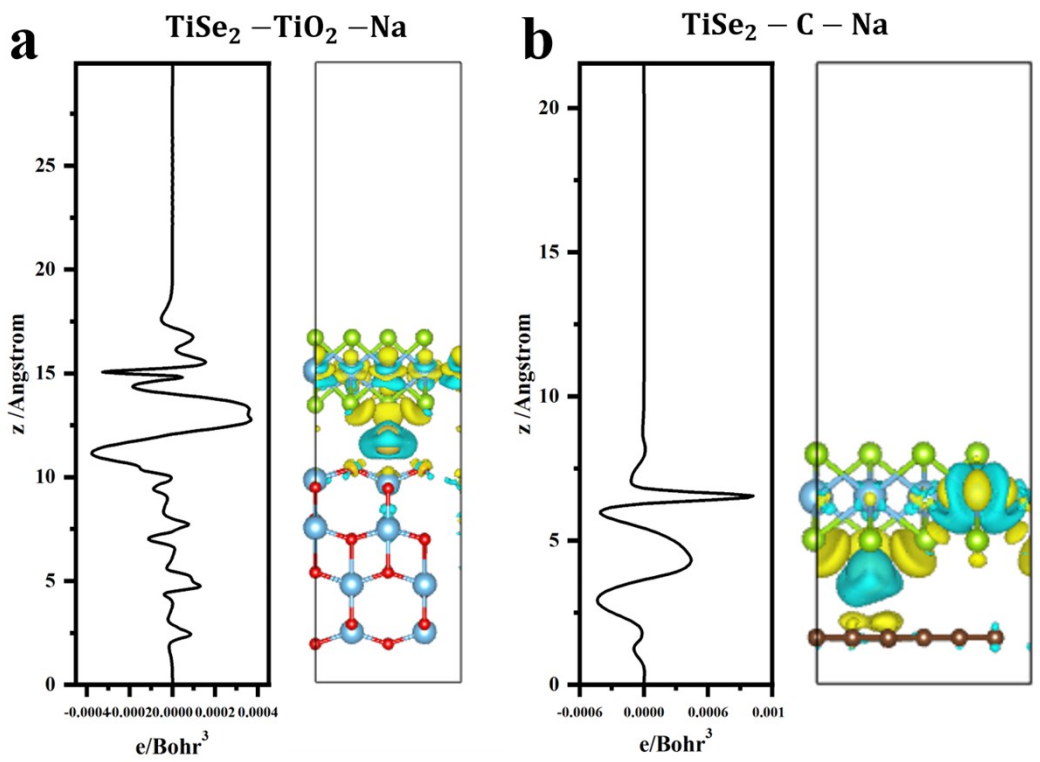

Figure S13. Planar electrostatic potential and charge difference of (a) $TiSe_2$-TiO_2-Na, (b) $TiSe_2$-C-Na.

Table S1. Crystallographic parameters of $TiSe_2$ for $TiSe_2$-Cl and $TiSe_2$-F refined by Rietveld method.

$TiSe_2$-Cl	$TiSe_2$ Space Group $P\bar{3}m1$			
	atom	x	y	z
	Ti	0.0	0.0	0.0
	Se	0.3333	0.6667	0.25691(29)
	a=*b*= 3.53573 Å *c*= 6.0061(5) Å *α*=*β*= 90º *γ*=120º *V*= 65.025(13) $Å^3$			
$TiSe_2$-F	$TiSe_2$ Space Group $P\bar{3}m1$			
	atom	x	y	z
	Ti	0.0	0.0	0.0
	Se	0.3333	0.6667	0.2588(10)
	a=*b*= 3.53561 Å *c*= 6.0066 Å *α*=*β*= 90º *γ*=120º *V*= 65.026(12) $Å^3$			
	TiO_2 Space Group I 41/a m d Z			
	atom	x	y	z
	Ti	0.0	0.25	0.375
	O	0.0	0.25	0.1687(6)
	a=*b*=3.78635 Å *c*=9.5114(6) Å *α*=*β*=*γ*=90º *V*=136.360(13) $Å^3$			

Table S2. Binding energy of Ti 2p, and Se 3d of $TiSe_2$-Cl and $TiSe_2$-F.

Ti 2p						
	$TiSe_2$		TiO_2		TiO_xSe_{2-x}	
$TiSe_2$-Cl	455.69	461.76	459.2	464.9	456.59	463.29
$TiSe_2$-F	455.73	461.73	459.03	464.91	456.46	463.02
Se 3d						
	t-Se		TiO_xSe_{2-x}		$TiSe_2$	
$TiSe_2$-Cl	55.56		54.65		53.42	54.25
$TiSe_2$-F	55.82		55.09		53.45	54.26

Units: eV

Table S3. Fitting results of EIS analysis for $TiSe_2$-Cl, $TiSe_2$-F, TiO_xSe_{2-x}-Cl, and TiO_xSe_{2-x}-F

	L (nH)	R_1 (Ω)	R_2 (Ω)	CPE_1		CPE_2	
				V (μF)	m	V (μF)	m
$TiSe_2$-Cl	290	1.83	1.86	580	965	20.8	645
$TiSe_2$-F	274	2.15	1.64	546	926	14.3	843

References

1. Y. Li, H. Shao, Z. Lin, J. Lu, L. Liu, B. Duployer, P. O. Å. Persson, P. Eklund, L. Hultman, M. Li, K. Chen, X.-H. Zha, S. Du, P. Rozier, Z. Chai, E. Raymundo-Piñero, P.-L. Taberna, P. Simon and Q. Huang, *Nat. Mater.*, 2020, **19**, 894-899.
2. M. Alhabeb, K. Maleski, B. Anasori, P. Lelyukh, L. Clark, S. Sin and Y. Gogotsi, *Chem.Mat.*, 2017, **29**, 7633-7644.
3. P. Giannozzi, O. Andreussi, T. Brumme, O. Bunau, M. Buongiorno Nardelli, M. Calandra, R. Car, C. Cavazzoni, D. Ceresoli, M. Cococcioni, N. Colonna, I. Carnimeo, A. Dal Corso, S. de Gironcoli, P. Delugas, R. A. DiStasio, A. Ferretti, A. Floris, G. Fratesi, G. Fugallo, R. Gebauer, U. Gerstmann, F. Giustino, T. Gorni, J. Jia, M. Kawamura, H. Y. Ko, A. Kokalj, E. Küçükbenli, M. Lazzeri, M. Marsili, N. Marzari, F. Mauri, N. L. Nguyen, H. V. Nguyen, A. Otero-de-la-Roza, L. Paulatto, S. Poncé, D. Rocca, R. Sabatini, B. Santra, M. Schlipf, A. P. Seitsonen, A. Smogunov, I. Timrov, T. Thonhauser, P. Umari, N. Vast, X. Wu and S. Baroni, *J. Phys.-Condes. Matter*, 2017, **29**, 465901.
4. M. Dion, H. Rydberg, E. Schröder, D. C. Langreth and B. I. Lundqvist, *Phys. Rev. Lett.*, 2004, **92**, 246401.
5. G. Henkelman, B. P. Uberuaga and H. Jónsson, *The J. of Chem. Phys.*, 2000, **113**, 9901 -9904.